
Article:
Raza, MA and Westwood, A orcid.org/0000-0002-5815-0429 (2019) Thermal contact resistance of various carbon nanomaterial-based epoxy composites developed for thermal interface applications. Journal of Materials Science: Materials in Electronics, 30 (11). pp. 10630-10638. ISSN 0957-4522

https://doi.org/10.1007/s10854-019-01408-8

THERMAL CONTACT RESISTANCE OF VARIOUS CARBON NANOMATERIAL-BASED EPOXY COMPOSITES DEVELOPED FOR THERMAL INTERFACE APPLICATIONS

Mohsin Ali Raza[1*], Aidan Westwood[2]

[1] Department of Metallurgy and Materials Engineering, CEET, University of the Punjab, Lahore, Pakistan
[2]School of Chemical and Process Engineering, University of Leeds, LS2 9JT, UK

*Corresponding author's e-mail: mohsin.ceet@pu.edu.pk

Abstract

Thermal interface materials (TIMs) are a vital component of electronic packaging as they facilitate heat removal from microchips by improving thermal contacts between the mating surfaces of chip and heat-sink. Filler-based polymer composite TIMs are utilized either as adhesives or pastes in electronic packaging. Carbon nanomaterials such as carbon nanotubes, graphite nanoplatelets (GNPs), few layered-graphene nanosheets (FLG) and carbon nanofibers have been extensively studied as fillers for the development of thermal interface adhesives or pastes due their high thermal conductivity. This work compares the thermal contact resistance (TCR) of epoxy composites incorporating FLG, GNPs or multiwalled carbon nanotubes (MWCNTs) under comparable conditions. GNPs and FLGs were produced by treating graphite flakes and graphite powder, respectively, via the Hummers' process followed by thermal reduction. Commercial MWCNTs and GNPs as well as in house-synthesized FLG and GNPs were dispersed into rubbery epoxy at 4 wt.% (2.1 vol.%) by a combined sonication and solvent mixing technique. The morphology of the fillers and resulting composites was studied by electron microscopy. The TCR of these composite TIMs, as adhesive coatings, was studied according to the ASTM D5470 method. The results showed that the TCR of MWCNT-epoxy composites increased with increase of MWCNT loading from 1 to 8 wt.%. The TCR of 1 wt.% MWCNT/rubbery epoxy composite was found to be 1.05×10^{-4} m^2.K/W at a bond line thickness of 15 µm, which was significantly higher than the value for corresponding FLG and GNP-based composites. The lowest TCR of 1.9×10^{-5} m^2.K/W at bond line thickness of 18 µm was obtained from the in-house GNP-based composite, half that of the corresponding FLG-

based composite, and this was attributed to the less defective structure of the in-house GNP compared to FLG. Thus, epoxy composites developed with in-house synthesized GNPs offer higher heat dissipating capability than commercial GNP-, MWCNT- or FLG-based epoxy composites.

1. Introduction

Thermal interface materials (TIMs) play important role in electronic packaging as they facilitate heat removal from microchips by improving thermal contacts between the mating surfaces of chip and heat-sink [1, 2]. Desired key characteristics of filler-based polymer composite TIM adhesives or pastes are high thermal conductivity, low thermal contact resistance (TCR), moderate viscosity, ease of application [3], good compliance, etc.

Carbon nanomaterials such as carbon nanotubes, graphite nanoplatelets (GNPs), few layered-graphene nanosheets (FLG), vapour grown carbon nanofibers (VGCNF) and carbon black (CB) have been studied extensively for thermal interface applications primarily due to their high thermal conductivity [4-7]. Among these carbon nanomaterials, GNPs enabled the composites with the highest thermal conductivities, for instance, a GNP/epoxy composite reported by Debalak and Lafadi [8] had thermal conductivity of 4 W/m.K, and GNP/rubbery epoxy composites reported by us [9] had thermal conductivity of 3.5 W/m.K obtained at loading of 20 wt.%. On the other hand, VGCNFs offers lower thermal conductivities than GNPs, but relatively higher thermal conductivities than MWCNTs. VGCNF/epoxy composite reported by Patton et al. [10] had thermal conductivity of 0.8 W/m.K at loading of 55 wt. %, we achieved similar thermal conductivity at much lower loading of filler (15 wt. %). The maximum thermal conductivity of VGCNF/rubbery epoxy composite produced by 3-roll mill at loading of 40 wt.% was 1.85 W/m.K. On the other hand, thermal conductivity of MWCNT/epoxy composite reported by Thostenson et al. [11] is half (0.35 W/m.K) than the VGCNF/epoxy composite reported by us [12] which was produced by 3-roll mill at equivalent loading of 5 wt.%. In contrast, CB cannot produce much improvement on the thermal conductivity of the polymers due to its amorphous and 0-D morphology. We reported maximum thermal conductivity of 0.3 W/m.K for CB/epoxy composite produced at 8 wt.% loading [13]. It is

clear from the published data that 2-D (GNP) and 1-D (CNT and VGCNF) carbon nanomaterials can improve thermal conductivity of insulating polymers appreciably, with data suggesting GNPs are more superior in improving the thermal conductivity of polymers.

Another 2-D carbon material, graphene, an atomic layer of sp^2 bonded carbon atoms, has greatly impacted the materials' research. Commercial graphene has thickness of 1-3 nm corresponding to 3-10 atomic layers of graphene [14]. Graphene with thickness in the range of 1-6 nm may be termed few-layered graphene (FLG). On the other hand, GNPs as discussed above are much thicker, with thickness in the range of 10-100 nm [15]. Both graphene and GNPs can be derived from graphite using top-down approach followed by Hummers' method [16] and acid intercalation method [17], respectively. The primary difference between graphene and GNPs is the thickness of the platelets. Graphene has enormous surface area (2700 m^2/g) which can certainly be very effective in occupying a large volume in the polymer matrix at relatively lower concentration resulting in formation of interconnecting networks required for the thermal transport.

Apart from filler's inherent thermal conductivity, several factors are influential in improving the thermal conductivity of polymer composites including processing techniques responsible for fillers' effective dispersion and distribution in the polymer matrix, fillers concentration, fillers morphology, polymer (resin) viscosity, fillers' surface treatment/functionalization, dispersing agent, curing temperature of the resin, etc. [18, 19]. These factors must be kept constant while comparing various carbon nanomaterials' properties and performance as filler for polymer composites.

A key criterion for qualifying performance of TIMs is the TCR (- the inverse of TCR is the thermal contact conductance). A low value of TCR indicates that a TIM has effectively filled air gaps between the mating surfaces resulting in an efficient transport of heat across the interface. Few papers have reported TCR data of polymer composites. TCR of various thermal pastes was reported by [20-24]. Lin et al. [24] reported a TCR of 1.67×10^{-4} m^2.K/W for GNP-paste at a thick bond line thickness of 50 µm, which was found half that of carbon black-paste. Recently, Lee et al. [25] studied the effect of residual oxygen groups on the TCR of reduced graphene oxide (rGO)/silicone

composites. They found that a TCR of 1.8 × 10^{-3} m^2.K/W was obtained from 2 wt.% rGO/silicone composite, about 40 % of the corresponding TCR of neat silicone. The authors reported that thermal reduction introduced phenolic groups on rGO which enabled improved dispersion of rGO in the silicone matrix. In recent years our group has also reported TCRs of polymer composites as adhesives [26], pastes [27] and pads [9].

This work compares heat dissipating performance by measuring the TCR of epoxy composites as thermal interface adhesives, prepared by incorporating few-layered graphene (FLG), GNPs or multiwalled carbon nanotubes (MWCNTs) under similar conditions and at similar loadings to determine which nanomaterial is the most effective filler for a thermal interface adhesive. In addition, thermal interfacial performance of materials developed in this work will be compared with commercial TIMs and those reported by other researchers. TCR is a measure of thermal impedance of the material which is directly proportional to thickness of the material. Higher TCR corresponds to lower heat transporting ability of the material. Thus, measuring TCR as a function of thickness helps to understand thermal response of composite/coating, and from the slope of the curve (TCR vs thickness) thermal conductivity of the composite can also be determined. TCR in this work was measured using a guarded hot plate method according to ASTM D5470 [26].

2. Materials and methods

Epoxy matrix used in this work was of rubbery nature which was developed by mixing epoxy resin (Epon 828, Hexion Specialty Chemicals) and polyetheramine hardener (Jeffamine D2000, ex Huntsman Corporation) at 1:3 and is named as rubbery epoxy (REP) [28]. Two different graphite precursors, graphite flakes (diameter ca. 0.5-2 mm) and powder (ca. 100-200 µm), were used to produce GNPs and FLG, respectively, employing a well-known Hummers' method followed by thermal exfoliation/reduction at 900 °C for 60 s under flowing nitrogen [29]. Commercial GNPs (XG Sciences, USA) and MWCNTs (Wuhan University of Science and Technology, China) were also used to produce composites for comparison.

Composites were developed by combined sonication and solvent mixing method (CSS). Briefly,

commercial GNPs (CGNP), in-house synthesised GNPs (IGNP), FLG, MWCNT powder were added into acetone at a concentration of 130 mg/100 ml along with appropriate amount of REP resin. This dispersion was ultrsonicated (80 W, 45 kHz) for 7-8 h at room temperature. After sonication, the acetone was evaporated under continuous magnetic stirring. The resulting carbon nanomaterials' dispersions were tested in a TCR measurement rig, designed according to ASTM D5470 [26]. Briefly, the rig consisted of two copper cylinders (diameter 30 mm and height 40 mm) with two holes (3 mm diameter) precisely machined in each cylinder for the insertion of RTD probes for temperature measurement. The copper cylinders were polished and had smooth surfaces with an average roughness of 0.06 µm, measured using a profilometer (Rank-Taylor Hobson, UK). The composite dispersion was coated on one of the cylinders using a spatula and then the other cylinder was placed on it to sandwich the coating. The coating-sandwiched cylinders were left for 1 h , with one cylinder above the other, to allow the excess coating to "leak" out from the interface. Afterward, these cylinders were heated in an oven at 120 °C for 3 h to allow the epoxy to cure. After curing, the cylinders were strongly adhered. The carbon nanomaterial-based epoxy composite-bonded cylinders were placed between hot and cold platens of a TCR measurement rig. The heater was turned on to the main temperature of 40 °C. The temperature of the cold plate was varied to achieve steady state condition, that is the temperature differences (i) between the two probes in the top cylinder and (ii) between the two probes in the bottom cylinder were almost the same. The values of temperatures were noted and TCR was determined using the equations reported in [26]. All measurements were carried out at an applied pressure of 0.032 MPa. After TCR measurement, samples were de-bonded and the coating thickness was measured accurately by a Talysurf profilometer. This was done by removing part of the coating from the surface to expose the copper surface. The stylus of the profilometer was scanned on the coating to the bare exposed copper. The "step" should be the height from bare copper on one cylinder to a point on the coating that had de-bonded-bonded fully (i.e., leaving only bare copper behind on the other cylinder). The step was taken as the bond line thickness of the coating. All composites were developed at a loading of 4 wt.%

(2.1 vol.%) for comparative analysis. MWCNT dispersions were also developed at 1 wt. % (0.5 vol.%) and 8 wt. %. (4.3 vol.%). Two commercial TIMs, Matrix^{TM} paste and EPM 2490 adhesive, were also tested for comparison in the TCR rig under similar conditions as used for the carbon nanomaterial-based epoxy composites. Matrix^{TM} is a commercial thermal paste comprised of zinc oxide, aluminium oxide and aluminium particles dispersed in silicone based oil, marketed by Arctic Silver Incorporated, USA. EPM 2490 is a thermal interface adhesive composed of 65 wt.% BN particles dispersed in silicone resin and marketed by Nusil Technology, USA.

Scanning electron microscopy (SEM, (LEO 1530)) was used to study morphology of carbon nanomaterials and their respective composites. Transmission electron microscopy (TEM, (FEI, Technai TF200) was used to measure thickness/diameter of GNPs, FLG and MWCNTs. Raman spectroscopy was employed to study structural disorder in GNPs and FLG-based composites.

3 Results and discussion

3.1 Morphology of carbon nanomaterials

Morphologies of IGNPs, FLG and MWCNTs are presented in Fig. 1. The average lateral size of IGNP and FLG was found to be 15 and 5 µm, respectively, as determined by SEM. The CGNPs had average lateral particle size of 15 µm, as reported in our previous work [28]. The thickness of these GNPs was measured using TEM analysis. The average thicknesses of CGNPs, IGNP, FLG were found to be 30, 20 and 5 nm, respectively. TEM image of MWCNTs is also presented in Fig. 1. The MWCNTs have diameter and length in the range of 25-45 nm and 1-10 µm, respectively. These nanotubes have herringbone like morphology (inset in Fig. 1 (c)).

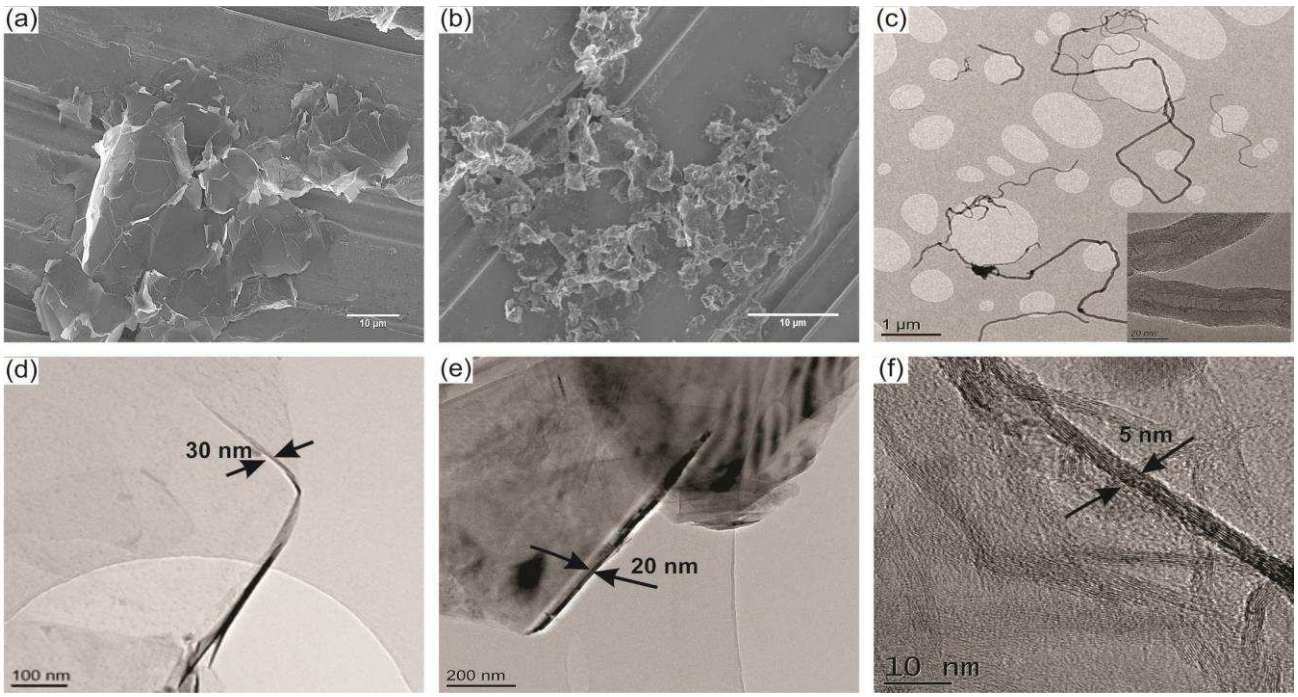

Fig. 1. SEM images of IGNP and FLGNP (a & b), TEM images of MWCNTs (inset shows herringbone like morphology of CNTs) (c), CGNP (d) IGNP (e) FLG (f)

3.2 TCR of GNP/FLG-based REP composites

The TCRs of 4 wt.% FLG/REP and 4 wt.% IGNP/REP composite coatings measured as an adhesive layer between the copper cylinders having smooth surface (Ra = 0.03 µm) at compressive stress of 0.032 MPa and temperature of ~25 °C are presented in Fig. 2 and Table 1. The TCR of composite produced with CGNP at 4 wt.% loading is also presented in Table 1.

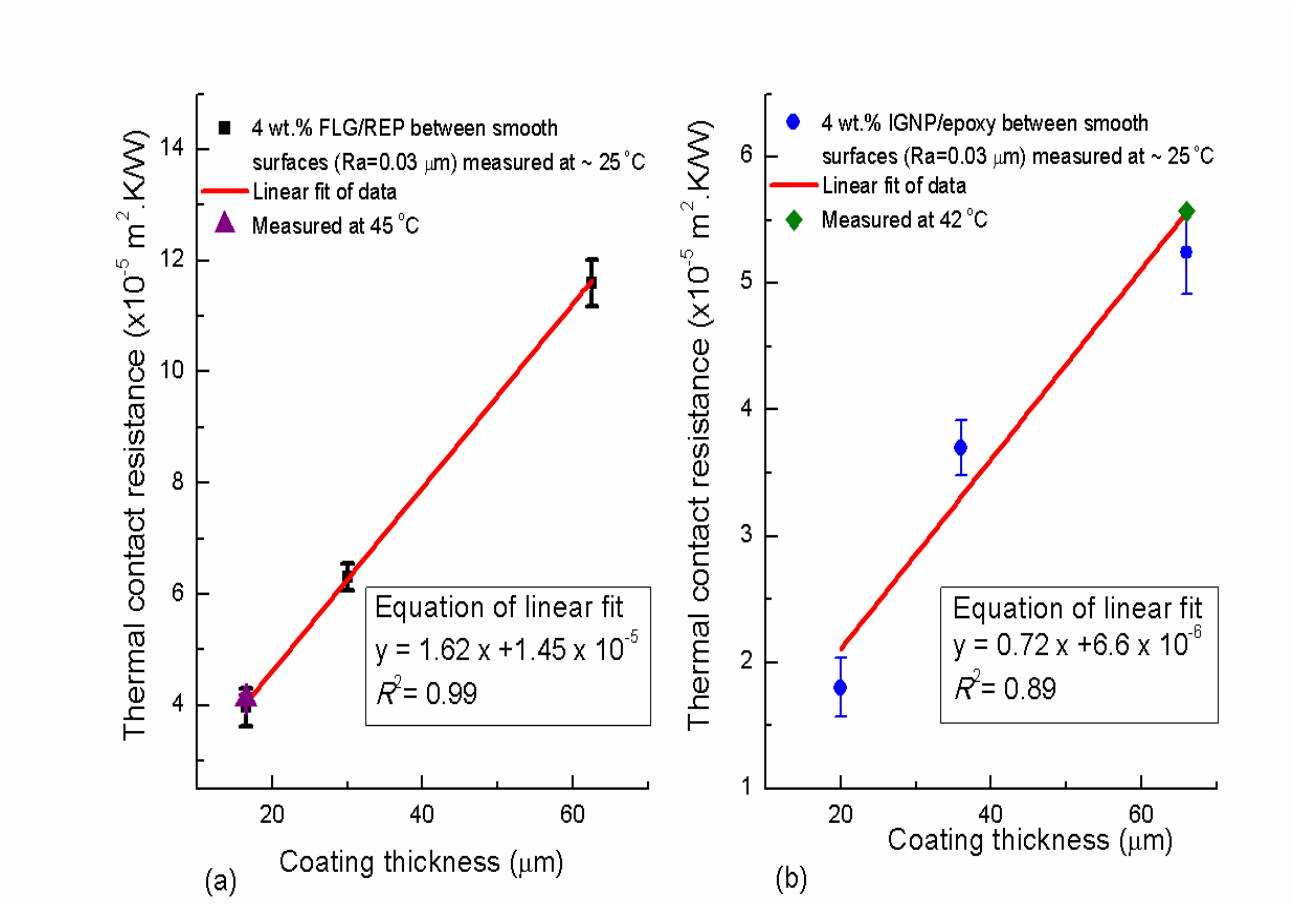

Fig. 2. TCR vs. coating thickness of (a) 4 wt.% FLG/REP and (b) 4 wt.% IGNP/REP composites measured between smooth surfaces (Ra = 0.06 μm) at ~0.032 MPa compressive stress and ~ 25 ℃. The effect of temperature on thermal contact resistance is also presented in Fig. 2. Eqs. of linear fit to data are also presented. Errors are obtained from at least 20 data points recorded under steady state conditions of 20-40 min.

It can be observed from Fig. 2 that very thin bond lines were obtained for both FLG and IGNP-based composite coatings. The TCR of both FLG and IGNP composite coatings remained almost the same with the increase of temperature from 25 to ~45 °C. It can be seen from Table 1 that at equivalent bond line thickness of ~23 μm the TCR of 4 wt.% FLG/REP and 4 wt.% CGNP/REP composites is ~2.3× higher than the 4 wt.% IGNP/REP composite. The TCR data suggests superiority of IGNPs over FLG and CGNPs. The better thermal transport performance of the 4 wt.% IGNP/REP composite is also attributed to its ~2× higher thermal conductivity (1.4 W/m.K, according to steady state method (inverse of slope in Fig. 2)) than corresponding FLG/REP composite (0.6 W/m.K). The TCR of 4 wt.% IGNP/REP composite is also slightly lower than 15 wt.% CGNP/REP composite produced by roll mill (Table 1) [9], indicating slightly better interfacial thermal transport performance of the former. The thermal conductivity of the 4 wt.% IGNP/REP composite (according to steady state method) is slightly higher than 15 wt.% GNP-15/rubbery epoxy composite reported in our previous publication [9] but obtained at 11 wt.% lower loading of GNPs. Thus, IGNPs offer higher thermal conductivities and lower TCR as

fillers in composites compared to CGNPs and FLG. These results certainly suggest that IGNPs are much better in quality than FLG and CGNPs and these could be much better fillers for TIMs.

Table 1. TCR GNP or FLG/REP composites measured at temperature of ~25 °C and compressive stress of 0.032 MPa at bond line thickness of ~23 ± 5 µm.

Composite coating	Total thermal contact resistance $m^2.K/W$
4 wt.% IGNP/REP	2.3×10^{-5}
4 wt.% FLG/REP	5.2×10^{-5}
4 wt.% CGNP/REP	5.1×10^{-5}
15 wt.% GNP-15/rubbery epoxy [9]	2.6×10^{-5}

The superior performance of IGNP over FLG can be attributed to the former's higher structural order and flatter surface morphology (Fig. 1 (d-e)). Raman spectra of IGNP/RE, FLG/REP and CGNP/REP are presented in Fig. 3. FLG showed higher intensity of D peaks and a shift of 10 cm^{-1} in 2D peak compared to IGNP and CGNP suggesting higher structural disorder in FLG [30]. On the other hand, CGNP displayed higher structural order than IGNP as can be seen from the higher ratio of intensities of G to D peak of the former cf. the latter.

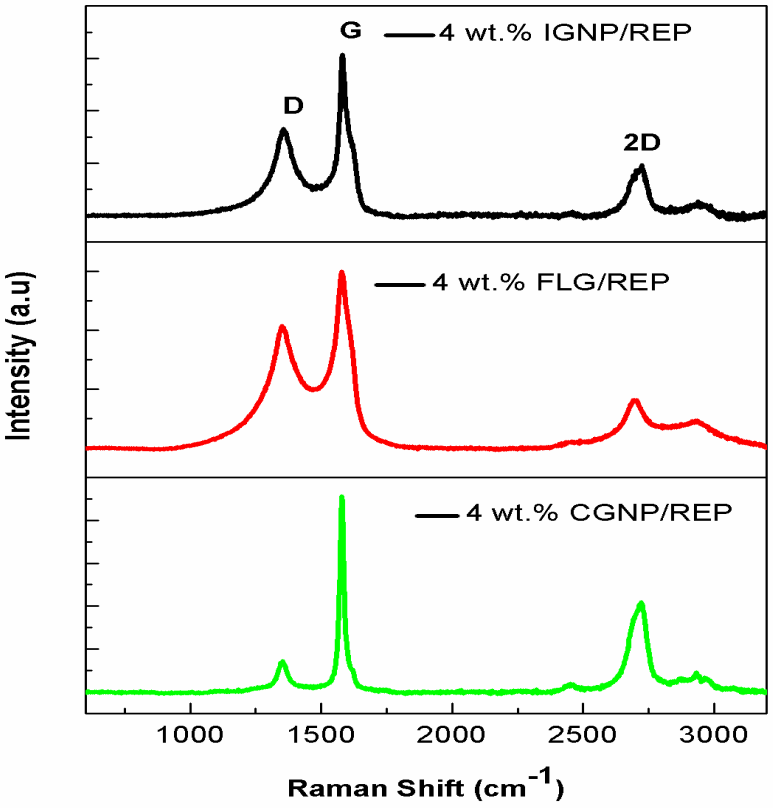

Fig. 3. Raman spectra of FLG/GNP-based REP composites

IGNP despite its higher structural disorder than CGNP gave better thermal transport performance as adhesive. This might be due to much higher surface area of IGNP (BET surface area = 200 m^2/g) than CGNP (BET surface area = 55 m^2/g), due to which former occupied much higher volume in the REP matrix resulting in the development of interconnects between IGNPs required for the better thermal conductance. This effect can be confirmed from SEM images of these composites shown in Fig. 4. It can be seen from the SEM image (Fig. 4 (b)) of the IGNP composite that GNPs are mostly visible and very less matrix can be observed between the GNPs. In contrast, CGNP composites showed fewer GNPs particles with no or little interconnects resulting in poor heat dissipation ability (Fig. 4(b)). On the other hand, FLG showed good dispersion and high volume in the matrix (Fig. 4(a)), however, these were not able to offer superior thermal transport ability mainly due to their much higher structural disorder than GNPs as confirmed by Raman spectroscopy (Fig. 3).

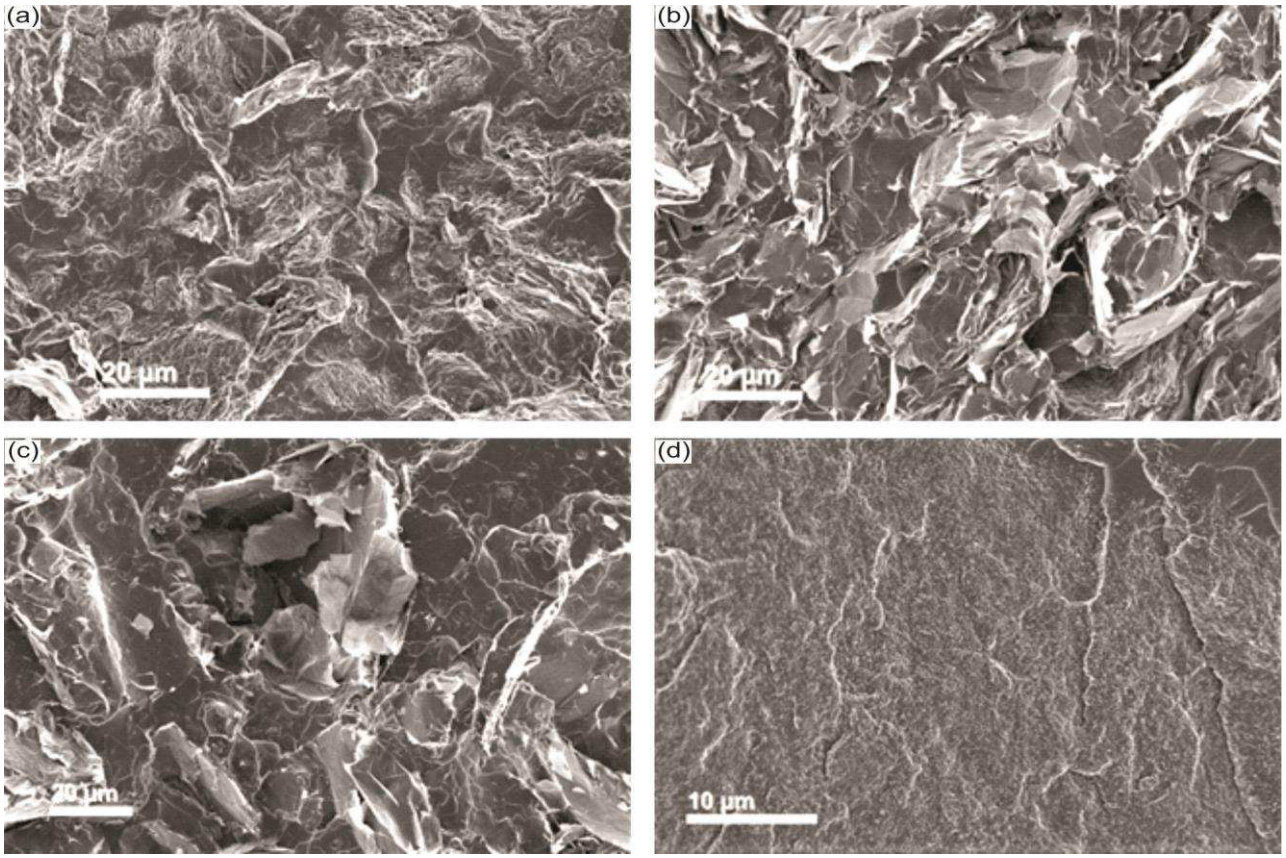

Fig. 4. SEM images of (a) 4 wt.% FLG/REP, (b) IGNP/REP, (c) CGNP/REP and (d) MWCNT/REP composite. Coating of the composite was removed from the copper substrate after the thermal contact resistance test and was freeze-fractured for SEM examination.

3.3 MWCNT/REP composites

MWCNT/REP composites were produced by CSS method at loadings of 1, 4 and 8 wt.% (loadings

higher than 8 wt.% were not possible as the mixture became too viscous). The performances of these composites as thermal interface adhesives were studied by measuring their TCR between copper surfaces. The effect of MWCNT loading on the TCR was investigated. The performance of MWCNT/REP composites as TIM adhesives was compared with other carbon nanofiller/REP composites.

The biggest challenge in producing high performance CNT/polymer composites lies in effectively dispersing the CNTs in the polymer matrix. The combined sonication and solvent mixing method produced composites with a good dispersion of CNTs as can be seen from Fig. 4 (d).

The TCR of the MWCNT/REP composites as thermal interface adhesives was studied between smooth copper surfaces. The viscosity, and therefore the bond line thickness, of MWCNT/REP composite increases with increasing wt.% of MWCNT. A minimum bond line thickness of ~15 µm was obtained with the composite produced at 1 wt.% loading, whereas the composites produced at 4 and 8 wt.% loading had minimum bond line thicknesses of ~30 and 70 µm, respectively, when applied under similar conditions on the copper substrate.

The TCR of MWCNT/REP composite adhesives (produced at 1, 4 and 8 wt.% loading) versus coating thickness measured between smooth copper surfaces (Ra = 0.06 µm) at ~25 °C and 0.032 MPa compressive stress is presented in Fig. 5.

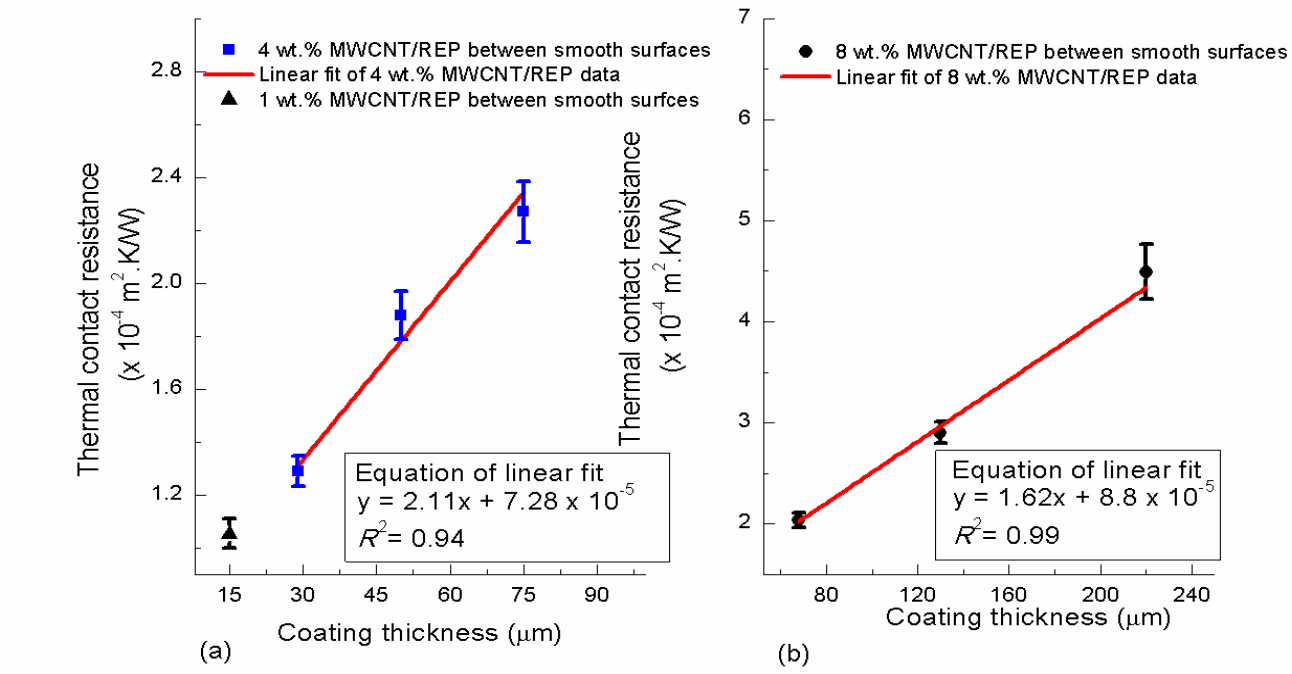

Fig. 5. TCR versus coating thickness of MWCNT/REP at (a) 4 wt.% (b) 8 wt.% MWCNT loading measured between smooth copper surfaces (Ra= 0.06 µm) at ~25 °C and 0.032 MPa compressive stress. The linear fit of data and equation of linear fit are also presented. The thermal contact resistance of 1 wt.% MWCNT/REP composite measured under the same conditions is also presented in (a). Errors are obtained from at least 20 data points recorded under steady state conditions of 20-40 mins.

The TCR of 1 wt.% MWCNT/rubbery epoxy composite is 1.05×10^{-4} m^2.K/W at a bond line thickness of 15 µm. MWCNT/rubbery epoxy composites with 4 and 8 wt.% MWCNT loading cannot be easily applied as a thin bond line. However, estimated from their equations of linear fit (Eqs in Fig. 5), their TCRs at 15 µm bond line thicknesses would be 1.04×10^{-4} and 1.12×10^{-4} m^2.K/W, respectively. These values are similar to that obtained for 1 wt.% MWCNT/rubbery epoxy composite coating. The thermal contact resistance of MWCNT/rubbery epoxy is almost the same as that of pure rubbery epoxy at equivalent bond line thickness of 15 µm (Table 2). This clearly shows that the incorporation of MWCNTs into rubbery epoxy does not improve the interfacial thermal transport performance of rubbery epoxy. This result is contrary to those observed with composites developed with GNP or FLG. Both FLG and GNPs have higher aspect ratio which resulted in fewer interconnects between the filler and, as a result, thermal contact resistances between the filler particles was lower. On the other hand, due to their smaller diameter (ca. 25-45 nm), MWCNTs formed more interconnects with each other, resulting in lower heat transfer due to higher interfacial thermal resistance.

The thermal conductivity of MWCNT/REP increases with increasing MWCNT content. According to the steady state method (i.e. inverse of slope, Fig. 5 (a & b)) the thermal conductivities of the 4 wt.% and 8 wt.% MWCNT/REP composites are ~0.47 and 0.62 W/m.K, respectively. Their significantly higher thermal conductivity, therefore had little effect on their interfacial thermal transport performance compared with 1 wt.% MWCNT/rubbery epoxy composite coating at thin bond lines. This might be due to poor interfacial contact of the MWCNT/rubbery epoxy coatings at 4 and 8 wt.% owing to their significantly increased viscosity. The geometric interfacial contact resistance (intercept of the graph in Fig. 5) of 8 wt.% MWCNT/rubbery epoxy composite is 8.8×10^{-5} m^2.K/W, slightly higher than that of 4 wt.% MWCNT/rubbery epoxy composite (Fig. 5). These high values suggest that the interfacial contacts of MWCNT/rubbery epoxy coatings with the substrate are poor and this might have resulted in poor interfacial thermal transport performance for these coatings.

3.4 Comparison of MWCNT, FLG or GNP/REP composite TIMs with other TIMs

The comparison of MWNT/REP, FLG/REP, IGNP/REP and CGNP/REP composite adhesives with the commercial TIMs and literature data on TIMs is presented in Table 2. The TCR of commercial paste (Matrix^{TM}) was measured on the rig under the similar conditions as that of GNP/REP composites. This paste displayed a very low TCR (4.6×10^{-6} m^2.K/W) under a pressure of 0.032 MPa at ca. 10-20 µm bondline thickness. Previously, Lin et al. [31] reported nanoclay-based pastes which showed much lower TCR than those of carbon black-, fumed alumina- or graphite nanoplatelet-based pastes. As presented in Table 2, Lin et al. [31] reported TCR of 2.5×10^{-6}

m^2.K/W at a bond line thickness of 0.4 µm (submicron) for a paste consisting of 1 vol.% of Cloisite 15A clay dispersed in polyol ester as an organic carrier. The lower TCR (better thermal interfacial performance) of their nanoclay paste is attributed to better conformability of the paste compared with the Matrix^{TM} paste studied in this work. The Matrix^{TM} paste used silicone resin as carrier which has higher viscosity than the carrier used by Lin et al. [31] for the development of the clay-based paste. It was not possible for us to achieve a bondline thickness less than 10 µm for Matrix^{TM} paste. It should also be noted that the nanoclay paste reported by Lin et al. [31] exhibited higher TCR at a bond line thickness of 10 µm (estimated from the equation of linear fit given in [31]) than that of Matrix^{TM} at equivalent bond line thickness, and this is attributed to the lower thermal conductivity of the former cf. the latter. At thick bond lines, higher thermal conductivity is required from TIMs to improve heat transport across the interface.

The TCR of 4 wt.% IGNP/REP developed in this work is ~4.8× higher than the Matrix^{TM} paste at approximately equivalent bond line thickness. This shows that the IGNP/REP adhesive cannot outperform Matrix^{TM} paste. On the other hand, it can also be observed from Table 2 that TCRs of GNP and CB-pastes reported by Lin et al. [24] are 4× and 9×, respectively, higher than 4 wt.% IGNP/REP composite at a thick bond line of ~50 µm. This shows that IGNP/REP adhesives perform much better at thick bond lines. The thermal contact resistance of commercial BN/silicone TIM (EPM 2490) is 1.17× higher than 4 wt.% IGNP/REP composites at a bond line thickness of 95 µm. The interfacial thermal transport performance of GNP/RE composites as TIM adhesives is not only better than commercial adhesive but is also obtained at 50-60 % less loading of the filler.

The interfacial thermal transport performance of MWCNT/REP composite is significantly poorer (~4.8× higher thermal contact resistance at 30 µm bond line thickness) than that of 4 wt.% IGNP/REP composite. The latter has ~3× higher thermal conductivity and significantly lower geometric thermal resistance than the former and these factors combine to afford the latter substantially improved performance. The 4 wt.% MWCNT/REP also fails at thick bond line as it had 2.4× higher TCR than the commercial TIM (EPM 2490) (Table 2) at equivalent thickness of 95 µm, suggesting superior interfacial thermal transport performance of the latter.

Table 2. Comparison of thermal contact resistance of carbon nanomaterials-based rubbery epoxy composites with other TIMs.

TIM	Reference	Pressure (MPa)	Bond line thickness (μm)	Thermal contact resistance (m^2.K/W)
Matrix^{TM} paste (commercial TIM)	Measured in the lab under same conditions at which GNP/REP studied	0.032	10-20	4.6×10^{-6}
Nanoclay paste (Cloisite 15A in polyol ester carrier developed by Lin et al. [31]	Measured according to ASTM method D5470	0.46	0.4	2.5×10^{-6}
Nanoclay paste (Cloisite 15A in polyol ester carrier developed by Lin et al. [31]	Estimated from the equation of linear fit reported by the authors in [31]	0.46	10	1.36×10^{-4}
Solder-graphite network composite developed by Sharma et al. [32]	Measured according to ASTM method D5470	0.46	50	3.82×10^{-6}
4 wt.% (2.1 vol.%) IGNP/REP	Present study (predicted on the basis of linear fit equation in Fig. 2)	0.032	18	1.9×10^{-5}
4 wt.% (2.1 vol.%) MWCNT/REP	Present study (predicted on the basis of linear fit equation in Fig. 2)	0.032	18	1.0×10^{-4}
15 wt.% (8.5 vol.%) GNP-15/rubbery epoxy adhesive	[9]	0.032	18	2.2×10^{-5}
2.4 vol. % GNP-paste	Estimated from the linear fit equation given in the reference [24]	0.46	18	4.45×10^{-5}
2.4 vol.% carbon black (Tokai) paste	Estimated from the linear fit equation given in the reference [24]	0.46	18	1.37×10^{-4}
2.4 vol.% GNP-paste	[24]	0.46	50	1.12×10^{-4}
2.4 vol.% carbon black (Tokai) paste	[24]	0.46	50	3.67×10^{-4}
15 wt.% (8.5 vol.%) GNP-15/rubbery epoxy adhesive	[9]	0.032	50	5.4×10^{-5}
4 wt.% (2.1 vol.%) IGNP/REP	Present study (predicted on the basis of linear fit equation)	0.032	50	4.26×10^{-5}
4 wt.% (2.1 vol. %) FLG/REP	Present study (predicted on the basis of linear fit equation)	0.032	50	9.54×10^{-5}
4 wt.% (2.1 vol.%) IGNP/REP	Present study (estimated on the basis of linear fit equation)	0.032	95	7.5×10^{-5}
65 wt.% (45 vol.%) BN/silicone (EPM 2490) adhesive	[33]	0.032	95	1.01×10^{-4}

Sharma et al. [32] developed solder-graphite network composite sheets and reported their thermal contact conductance. These composite sheets were used to bond copper cylinders (used to study TCR) by melting. This was similar to our composites which acted as adhesives upon curing to bond copper cylinders. The TCR of the solder-graphite composite reported by Sharma et al. [32] is presented in Table 2. The authors reported a lowest TCR of 3.86×10^{-6} m^2.K/W at a bond line thickness of 50 µm for a solder-graphite composite. Our carbon nanomaterial-based epoxy composite adhesives had much higher TCR than solder-graphite composites. There may be two reasons for this difference; firstly the polymer composite adhesive (1.4 W/m.K) developed in this work had much lower thermal conductivity than the solder-graphite composite (more than 50 W/m.K) and secondly the solder-graphite composite, after melting, acquires better conformability with the copper surface, resulting in much more intimate interfacial contact than in the case of the polymer composite adhesives.

The composite materials developed in this work cannot surpass the performance of the commercial thermal paste (Matrix^{TM}), the nanoclay pastes reported by Lin et al. [31] or the graphite-solder composites reported by Sharma et al. [32] but their performance is comparable or perhaps better than other thermal pastes reported by Lin et al. [24] and the commercial thermal adhesive, EPM 2490, at equivalent bond line thickness. In fact, our highest performing material, 2.4 vol.% IGNP/REP, showed approximately an order of magnitude lower thermal contact resistance than thermal pastes at a large bond line thickness of 50 µm, which suggests that adhesives are more suitable for larger gap filling applications. Thermal interface adhesives are much more reliable than thermal pastes as their TCR does not change upon the application of low pressures [26] and, as a result, their heat dissipation ability will not be affected with time as there would be little or no chance of leakage of adhesives from the interfaces.

4. Conclusions

The composites produced with GNPs synthesized via Hummers' route followed by thermal reduction had superior heat transport performance as TIMs compared to the composites produced with commercial

GNPs at similar loading of 4 wt.%. The 4 wt.% IGNP/REP composite had higher thermal conductivity and lower TCR than the corresponding composite produced with FLGs and commercial GNP-15s. This is attributed to much flatter IGNPs, less structural disorder and presence of fewer functional groups on their surface compared to other FLG and commercial GNPs. The interfacial thermal transport performance of MWCNT/REP composite was inferior to GNPs and FLG-based epoxy composites might be due to incapacity of MWCNT to align perpendicular along the direction of heat flow. The ICGNP/REP composites can perform much better at thick bond lines as these outperformed commercial TIM adhesive.

Acknowledgement

The authors would like to thank Higher Education Commission of Pakistan (Grant No. 20-3283) for providing financial support for this work.

References

1. DDL Chung,Thermal Interface Materials. Journal of Materials Engineering and Performance **10**, 56-59 (2001)
2. NF Dean, AL Gettings,Experimental Testing of Thermal Interface Materials on Non-Planar Surfaces. Fourteenth IEEE SEMI-THERM™ Symposium 88-94 (1998)
3. DDL Chung, C Zweben, K Anthony, Z Carl (2000) Comprehensive Composite MaterialsPergamon, Oxford
4. A Yu, ME Itkis, E Bekyarova, RC Haddon,Effect of single-walled carbon nanotube purity on the thermal conductivity of carbon nanotube-based composites. APPLIED PHYSICS LETTERS **89**, 1-3 (2006)
5. A Yu, P Ramesh, ME Itkis, E Bekyarova, RC Haddon,Graphite Nanoplatelet−Epoxy Composite Thermal Interface Materials. J. Phys. Chem. C **111**, 7565-7569 (2007)
6. C-W Nan, G Liu, Y Lin, M Li (2004) AIP,
7. M Raza, A Westwood, C Stirling,Carbon black/graphite nanoplatelet/rubbery epoxy hybrid composites for thermal interface applications. Journal of Materials Science **47**, 1059-1070 (2012)
8. B Debelak, K Lafdi,Use of exfoliated graphite filler to enhance polymer physical properties. Carbon **45**, 1727–1734 (2007)
9. MA Raza, A Westwood, C Stirling,Graphite nanoplatelet/rubbery epoxy composites as adhesives and pads for thermal interface applications. Journal of Materials Science: Materials in Electronics **29**, 8822-8837 (2018)
10. RD Patton, JCU Pittman, L Wang, JR Hill,Vapor grown carbon fiber composites with epoxy and poly(phenylene sulfide) matrices. Composites Part A: Applied Science and Manufacturing **30**, 1081-1091 (1999)
11. ET Thostenson, T-W Chou,Processing-structure-multi-functional property relationship in carbon nanotube/epoxy composites. Carbon **44**, 3022-3029 (2006)
12. MA Raza, A Westwood, C Stirling,Effect of processing technique on the transport and mechanical properties of vapour grown carbon nanofibre/rubbery epoxy composites for electronic packaging applications. Carbon **50**, 84-97 (2012)
13. M Ali Raza, A Westwood, C Stirling, R Brydson, N Hondow,Effect of nanosized carbon black on the morphology, transport, and mechanical properties of rubbery epoxy and silicone composites. Journal of Applied Polymer Science **126**, 641-652 (2012)
14. AK Geim, KS Novoselov,The rise of graphene. Nat Mater **6**, 183-191 (2007)
15. B Li, W-H Zhong,Review on polymer/graphite nanoplatelet nanocomposites. Journal of Materials Science **46**, 5595-5614 (2011)
16. S Stankovich, DA Dikin, RD Piner, et al.,Synthesis of graphene-based nanosheets via chemical reduction of exfoliated graphite oxide. Carbon **45**, 1558-1565 (2007)
17. Y Geng, SJ Wang, J-K Kim,Preparation of graphite nanoplatelets and graphene sheets. Journal of Colloid and Interface Science **336**, 592-598 (2009)

18. MH Al-Saleh, U Sundararaj,A review of vapor grown carbon nanofiber/polymer conductive composites. Carbon **47**, 2-22 (2009)
19. BZ Jang, A Zhamu,Processing of nanographene platelets (NGPs) and NGP nanocomposites: a review. Journal of Materials Science **43**, 5092-5101 (2008)
20. C-K Leong, Y Aoyagi, DDL Chung,Carbon black pastes as coatings for improving thermal gap-filling materials. Carbon **44**, 435-440 (2006)
21. C-K Leong, Y Aoyagi, DDL Chung,Carbon-Black Thixotropic Thermal Pastes for Improving Thermal Contacts. Journal of Electronic Materials **34**, (2005)
22. C-K Leong, DDL Chung,Carbon black dispersions as thermal pastes that surpass solder in providing high thermal contact conductance. Carbon **41**, 2459-2469 (2003)
23. C Lin, D Chung,Nanostructured fumed metal oxides for thermal interface pastes. Journal of Materials Science **42**, 9245-9255 (2007)
24. C Lin, DDL Chung,Graphite nanoplatelet pastes vs. carbon black pastes as thermal interface materials. Carbon **47**, 295-305 (2009)
25. S-Y Lee, P Singh, RL Mahajan,Role of oxygen functional groups for improved performance of graphene-silicone composites as a thermal interface material. Carbon **145**, 131-139 (2019)
26. M Raza, A Westwood, A Brown, C Stirling,Performance of graphite nanoplatelet/silicone composites as thermal interface adhesives. Journal of Materials Science: Materials in Electronics 1-9 (2012)
27. MA Raza, A Westwood, C Stirling,Comparison of carbon nanofiller-based polymer composite adhesives and pastes for thermal interface applications. Materials & Design **85**, 67-75 (2015)
28. MA Raza, AVK Westwood, C Stirling,Effect of processing technique on the transport and mechanical properties of graphite nanoplatelet/rubbery epoxy composites for thermal interface applications. Materials Chemistry and Physics **132**, 63-73 (2012)
29. MA Raza, A Westwood, A Brown, N Hondow, C Stirling,Graphite Nanoplatelets Produced by Oxidation and Thermal Exfoliation of Graphite and Electrical Conductivities of Their Epoxy Composites. Journal of nanoscience and nanotechnology **12**, 9259-9270 (2012)
30. AC Ferrari, DM Basko,Raman spectroscopy as a versatile tool for studying the properties of graphene. Nature nanotechnology **8**, 235 (2013)
31. C Lin, D Chung,Nanoclay paste as a thermal interface material for smooth surfaces. Journal of electronic materials **37**, 1698-1709 (2008)
32. M Sharma, D Chung,Solder–graphite network composite sheets as high-performance thermal interface materials. Journal of Electronic Materials **44**, 929-947 (2015)
33. MA Raza, AVK Westwood, C Stirling, N Hondow,Transport and mechanical properties of vapour grown carbon nanofibre/silicone composites. Composites Part A: Applied Science and Manufacturing **42**, 1335-1343 (2011)